Asociación Argentina
de Mecánica Computacional

Mecánica Computacional Vol XXXIV, págs. 3383-3394 (artículo completo)
Sebastián Giusti, Martín Pucheta y Mario Storti (Eds.)
Córdoba, 8-11 Noviembre 2016

APPROXIMATE SOLUTIONS TO INTEGRAL EQUATIONS BY WAVELET DECOMPOSITION METHODS

María I. Troparevsky[a], **Eduardo P. Serrano**[b,c] **and Marcela A. Fabio**[c]

[a]*Departamento de Matemática, Facultad de Ingeniería, Universidad de Buenos Aires, Argentina, mariainestro@gmail.com*

[b]*Escuela Superior Técnica FE-UNDEF, Argentina, eduardo.eduser@gmail.com*

[c]*Centro de Matemática Aplicada, Universidad Nacional de San Martín, Argentina, celafabio@gmail.com*

Keywords: Integral Operators, Inverse Problem, Band Limited Wavelet, Multiresolution Analysis.

Abstract. We construct approximate solutions to Inverse Problems associated to equations of the form Af = g where A is an integral operator. For a given f , the Forward Problem consists in calculating its image through A, while the Inverse Problem looks for f for a given g. In order to solve the Inverse Problem we project the data into finite dimensional subspaces of wavelets in the context of a multiresolution analysis and solve the Foward Problem for each element of the basis by means of a Galerkin-type scheme. From these computations, we can accurately build a solution to the Inverse Problem based on properties of the chosen wavelets and suitable hyphotesis on the operator. We present examples related to fractional calculus.

1 INTRODUCTION

We consider Inverse Problems (IP) associated to equations of the form

$$Af(x) = \int_{\mathbb{R}} h(x,\omega)\widehat{f}(\omega)e^{i\omega x}d\omega = g(x), \quad x \in \mathbb{R} \tag{1}$$

with $\widehat{f}$ is the Fourier transform of $f \in L^2(\mathbb{R})$ and the kernel h is a bounded and Lipschitz continuous function with fast decay.

If we consider $k(x,y) = \int_{\mathbb{R}} h(x,\omega)e^{i\omega(x-y)}d\omega$, we can express the operator as

$$Af(x) = \int_{\mathbb{R}} k(x,y)f(y)dy \tag{2}$$

(see Kress (2014)).

In addition, if we suppose that the kernel h is symmetric in ω, i.e., $h(x,\omega) = h(x,-\omega)$, and verifies $|h(x,\omega)| \leq \frac{M}{(1+|x|)^{\frac{1+\varepsilon}{2}}(1+|\omega|)^{\frac{1+\varepsilon}{2}}}$, $M > 0$, $\varepsilon > 0$, we can assure that $A : L^2(\mathbb{R}) \to L^2(\mathbb{R})$.

For a given f, the Forward Problem (FP) associated to (1) consists in calculating its image g through A, while the IP looks for f for a given g. In the last decades decomposition methods were proposed to solve problems associated to integral operators (A. Cohen and Reiβ (2004), Dicken and Maaβ (2006), Donoho (1995)) and several techniques based on Wavelet Galerkin Methods and Wavelet Vaguelet Decomposition were developed. In (Serrano et al. (2014a)) and (Serrano et al. (2014b)) we studied the IP when A is a pseudo-differential operator. Under appropriate hypothesis on the kernel, the inverse of each element of a selected basis is calculated approximately. Discretization techniques were also developed.

In this work we construct approximate solutions to the IP associated to integral equations of the form (1). We choose an appropriate band limited wavelet basis, $\{\psi_{jk},\ k,j \in \mathbb{Z}\}$, associated to a Multiresolution Analysis (MRA) where, for each integer j, W_j denotes the wavelet space that naturally corresponds to a two side-band frequency set Ω_j (Walnut (2002), Mallat (2009)) and project the data g in finite dimensional wavelet subspaces. We solve first the FP calculating the image of each element of the basis. We recover the coefficients of the decomposition of f in those subspaces by means of a Galerkin scheme. Based on regularty assumptions on h and properties of the wavelets, the algebraic equations can be solved accurately and the solution to the IP on each level j is derived. The resulting scheme is simple and efficient.

In the next section we briefly describe the wavelet basis and the associated MRA. In Section 3 considerations on the data are stated and the approximate solution to the IP is developed in detail. Examples are introduced in Section 4. Finally we present some conclusions.

2 THE WAVELET BASIS

A wavelet is an oscillating function, well localized in both time and frequency domains. For special selection of the mother wavelet ψ the family $\{\psi_{jk}(x) = 2^{j/2}\ \psi(2^j x - k),\ j,k \in \mathbb{Z}\}$, is an orthonormal basis of $L^2(\mathbb{R})$, associated to a hierarchical structure of the space, i.e., a sequence of nested scale-subspaces V_j, called MRA (see Walnut (2002), Mallat (2009)) such that $L^2(\mathbb{R}) = \bigoplus_{j\in\mathbb{Z}} W_j = \bigoplus_{j\geq n} W_j + V_n$, for any $n \in \mathbb{Z}$.

For our purpose we choose a smooth, infinitely oscillating mother wavelet with fast decay $\psi \in \mathcal{S}$, the Schwartz class, well localized in both, time and frequency domain (see Meyer (1990)). Its spectrum $|\widehat{\psi}(2^{-j}\omega)|$ is supported on the two-sided band

$$\Omega_j = \left\{\omega : 2^j(\pi-\alpha) \leq |\omega| \leq 2^{j+1}(\pi+\alpha)\right\}$$

for some $0 < \alpha \leq \pi/3$. Figure 1 right and left, show the graph of ψ and $|\hat{\psi}|$ respectively. There

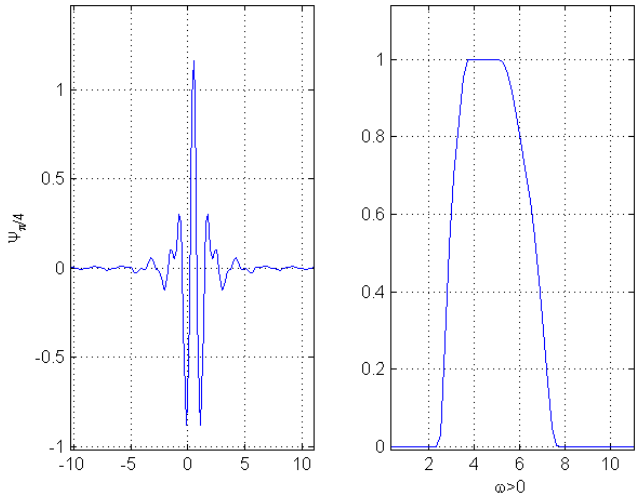

Figure 1: Mother wavelet for $\alpha = \pi/4$ and $|\widehat{\psi}|$ for $\omega \geq 0$

also exists $\phi \in V_0$ such that $\{\phi(x-k), k \in \mathbb{Z}\}$ is an orthonormal basis of V_0.

Let $W_j = \text{span}\{\psi_{jk}, k \in \mathbb{Z}\}$ and $V_J = \bigoplus_{j<J} W_j$, the wavelet and the scales subspaces. Each family $\left\{\phi_{Jn}(x) = 2^{J/2}\phi(2^J x - n), n \in \mathbb{Z}\right\}$ is an orthonomal basis of V_J.

For any signal $s \in L^2(\mathbb{R})$, we denote by $\mathcal{Q}_j s$ and $\mathcal{P}_j s$ their orthogonal projections on W_j and V_j, respectively. Then, the following representation holds

$$s(x) = \sum_{j\in\mathbb{Z}} \mathcal{Q}_j s(x) = \mathcal{P}_J s(x) + \sum_{j\geq J} \mathcal{Q}_j s(x) = \sum_{n\in\mathbb{Z}} \langle s, \phi_{Jn}\rangle \, \phi_{Jn}(x) + \sum_{j\geq J} \sum_{k\in\mathbb{Z}} \langle s, \psi_{jk}\rangle \, \psi_{jk}(x)$$

for any index J. We remark that $\widehat{\mathcal{Q}}_j s$ is supported on Ω_j and $\widehat{\mathcal{P}}_J s$ on $\cup_{j\leq J}\Omega_j$.

The properties of ψ ensure uniform convergence in each W_j. In addition, since ψ is infinitely oscillating, it has nulled moments $\int_{\mathbb{R}} x^n \psi(x)\, dx = 0$, $\forall n \in \mathbb{N}_0$, and the same occurs to its polynomials components.

The design of this basis and the implementation algorithm based on the Fast Fourier Transform have been developed by the authors in (Serrano et al. (2012)).

3 APPROXIMATE SOLUTIONS TO THE IP

3.1 The data

We suppose that $g(x) = \sum_{j=0}^{J} g_j(x) + r$ with $||r||_2 < \epsilon \|g\|_2 \cong 0$, $J \in \mathbb{N}$ and

$$g_j(x) = \sum_{k\in\mathbb{Z}} c_{jk}\psi_{jk}(x) \in W_j$$

where $c_{jk} = \langle g, \psi_{jk}\rangle$ are the wavelet coefficients.

If the data is a sampled function, a previous interpolation process must be carried out, in an adequate V_J, disregarding the low frequency components, i.e., $\widehat{\mathcal{P}}_J g$ is nearly zero.

We denote by $\tilde{g}_j$ the truncated projection of the data in W_j,

$$\tilde{g}_j(x) = \sum_{k \in \mathbb{K}_j} c_{jk} \psi_{jk}(x) \tag{3}$$

where $\mathbb{K}_j \subset \mathbb{Z}$, $|\mathbb{K}_j| = \kappa_j < \infty$, satisfying $\sum_{k \notin \mathbb{K}_j} |\langle g, \psi_{jk} \rangle|^2 < \epsilon ||g_j||^2$ with $\epsilon \cong 0$.

3.2 The approximated solution to the IP

Let

$$f(x) = \sum_{j \in \mathbb{Z}} \sum_{k \in \mathbb{Z}} b_{jk} \psi_{jk}(x) \tag{4}$$

and v_{jk} the images of the wavelet basis through the operator, i.e., $A\psi_{jk} = v_{jk}$, $k \in \mathbb{K}_j$

$$v_{jk}(x) = \int_{\Omega_j} h(x_j, \omega) \widehat{\psi}_{jk}(\omega)\, e^{i\omega x}\, d\omega. \tag{5}$$

Then, from (4)

$$Af(x) = \sum_{j \in \mathbb{Z}} \sum_{k \in \mathbb{Z}} b_{jk} v_{jk}(x) = \sum_{j' \in \mathbb{Z}} \sum_{k' \in \mathbb{Z}} c_{j'k'} \psi_{j'k'}(x) = g(x). \tag{6}$$

For each $0 \leq j \leq J$, we consider that $A(W_j) \cong W_j$, if this is not the case, we can proceed analogously considering an appropriate union of wavelet subsets. Regarding the truncated projection of the data, we restrict ourselves to $\mathbb{K}_j$. Then, for $m \in \mathbb{K}_j$, we obtain the normal equations

$$\left\langle \sum_{l \in \mathbb{K}_j} b_{kl} v_{jl}, \psi_{jm} \right\rangle = \sum_{l \in \mathbb{K}_j} b_{kl} \langle v_{jl}, \psi_{jm} \rangle = c_{jm},\ k \in \mathbb{K}_j. \tag{7}$$

We build the Grammian-type matrix $M^j \in \mathbb{R}^{\kappa_j} \times \mathbb{R}^{\kappa_j}$ that contains the inner products

$$M^j_{lm} = \langle v_{jl}, \psi_{jm} \rangle, \tag{8}$$

and look for the vector of coefficients satisfying

$$M^j \mathbf{b}^j_k = \mathbf{c}^j_k,\ k \in \mathbb{K}_j \tag{9}$$

where $\mathbf{b}^j_k = (b_{jk})_{k \in \mathbb{K}_j}$ and $\mathbf{c}^j_k = (c_{jk})_{k \in \mathbb{K}_j}$.

Then, ideally, we have to invert M^j, find the vectors $\mathbf{b}^j_k$ for each j and construct the approximate solution $\tilde{f} \cong f$,

$$\tilde{f}(x) = \sum_{0 \leq j \leq J} \tilde{f}_j(x) = \sum_{0 \leq j \leq J} \sum_{k \in \mathbb{K}_j} b_{jk} \psi_{jk}(x). \tag{10}$$

Note that it is not actually necessary to calculate v_{jk}, only the matrix M^j is needed. Since it depends only on the operator A and the wavelet basis, we can calculate it previously.

In the next subsection we developed a numerical approximation scheme to compute M^j that involves simple calculations.

3.3 The matrix M^j

In order to calculate the elements of M^j we need to integrate over Ω_j to obtain v_{jk} in (5) and afterwards on x over $\mathbb{R}$ to build M^j (8). However, based on regularity hypothesis on the kernel h and properties of the wavelets, we can accurately approximate these integrals as follows.

We consider that the kernel $h(x,\omega)$ is symmetric in ω and well localized on $I_{jk} = 2^{-j}[k, k+1]$, then for x in a neighbourhood of I_{jk} we have :

$$h(x,\omega) \cong h(x_{jk},\omega). \tag{11}$$

In addition, there exist $N \in \mathbb{N}$ and a net of frequencies such that the following representation holds

$$h(x_{jk},\omega) = \alpha_{0,k} + 2\alpha_{1,k}\cos(\omega/2^j) + \cdots + 2\alpha_{N,k}\cos(N\omega/2^j) + \epsilon(\omega), \tag{12}$$

where $\epsilon(\omega)$ is an error that is small for large N.

The coefficients $\alpha_{l,k}$ for $0 \le l \le N$ can be computed accurately from the values of h in the net.

Then, from (5), (11) and (12), we have

$$v_{jk}(x) \;\cong\; \int_{\Omega_j} \left(\alpha_{0,k} + 2\alpha_{1,k}\cos(\omega/2^j) + \cdots + 2\alpha_{N,k}\cos(N\omega/2^j)\right)\; \widehat{\psi}_{jk}(\omega)\; e^{i\omega x}\; d\omega.$$

We observe that, for $1 \le n \le N$

$$\begin{aligned} 2\alpha_{n,k}\cos(n\omega/2^j)\widehat{\psi}_{jk}(\omega) &= \alpha_{n,k}\left(e^{-in\omega/2^j} + e^{in\omega/2^j}\right)\widehat{\psi}_{jk}(\omega) \\ &= \alpha_{n,k}\left(e^{-in\omega/2^j} + e^{in\omega/2^j}\right)|\widehat{\psi}_j(\omega)|e^{(k+1/2)/2^j} \\ &= \alpha_{n,k}\left(\widehat{\psi}_{j(k-n)}(\omega) + \widehat{\psi}_{j(k+n)}(\omega)\right), \end{aligned}$$

then

$$v_{jk}(x) \cong 2\pi\alpha_{0,k}\psi_{jk}(x) + 2\pi\alpha_{1,k-1}\psi_{j(k-1)}(x) + 2\pi\alpha_{1,k+1}\psi_{j(k+1)}(x) + \cdots .$$

Finally, we can approximate for $0 \le m \le N$

$$\langle v_{jk}, \psi_{jm}\rangle \cong 2\pi\alpha_{m,k}. \tag{13}$$

The inner products are zero for $m > N$.

Thus, the matrix M^j is diagonal dominant. From (9), we obtain the coefficients $\mathbf{b}_k^j$ of $\tilde{f}_j$, (see (10)).

The accuracy of the the proposed approximation scheme can be improved since the errors introduced rely on the hypothesis on the localization of the h (see (11)) and on the computation of the coefficients $\alpha_{l,k}$ in (12).

3.4 Approximation errors

For the class of integral operators considered in this work, we have proposed an approximation scheme that introduces different kind of errors.

- In order to calculate $\mathbf{b}_\mathbf{k}^\mathbf{j}$, we have assumed that $A(W_j) \cong W_j$. If this is not the case, we can proceed analogously considering an appropriate union of wavelet subsets.

- On each level j, we only consider a finite set of integers, $k \in \mathbb{K}_j \subset \mathbb{Z}$, introducing an error that can be controlled. We do not consider the low frequency components.
- When we calculate the elements of M^j an approximation is performed. Its accuracy is assured by simmetry and localization hypothesis on h, and localization of the chosen wavelet basis in both time and frequency domains.

4 EXAMPLES

4.1 Estimate accuracy

For two operators with kernels (see Figure 2)

$$\begin{aligned} h_1(x,\omega) &= |\omega|^{0.4} \\ h_2(x,\omega) &= \frac{1}{1+2|x|^{0.5}+|\omega|^{0.4}}, \end{aligned}$$

we illustarte the accuracy of the approximation formula proposed in (13) and the matrix M^j.

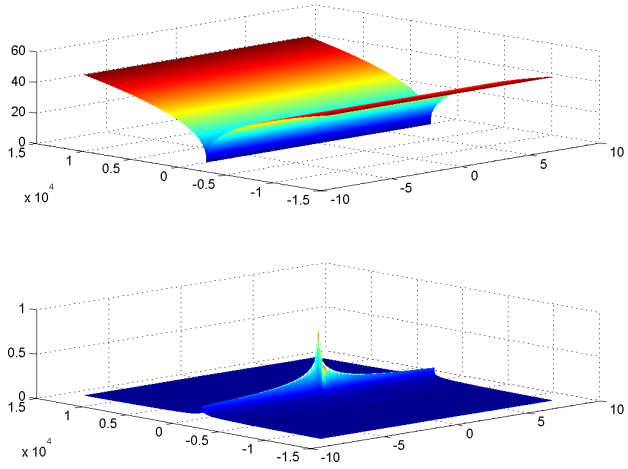

Figure 2: Kernels $h_1(x,\omega) = |\omega|^{0.4}$ (above) and $h_2(x,\omega) = \frac{1}{1+2|x|^{0.5}+|\omega|^{0.4}}$ (below)

In Figure 3 we show the plot of the function $v_{3,0}$ associated with h_1 (not depending on x) together with the plot of the wavelet $\psi_{3,0}$ and $v_{3,0}$, verifying that $v_{3,0} \cong 2\pi\psi_{3,0}h_1(\omega_3)$ with $\omega_3 = (3\pi/2)2^3$.

We generate a few functions v_{jk} associated with h_2, $j = 3$ and $k = 0, 5, 15$. We compare the plots of the wavelet $\psi_{3,0}$ and $v_{3,0}$. Once more, we observe that, $v_{3,0} \cong 2\pi\psi_{3,0}h_2(x_{3,0},\omega_3)$ with $\omega_3 = (3\pi/2)2^3$ and $x_{3,0} = (1/2)/2^3$ (see Figure 4).

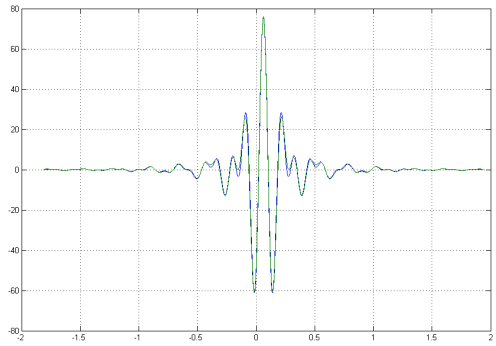

Figure 3: Functions $v_{3,0}$ (green) and $2\pi(1.5\pi 8)^{0.4}\psi_{3,0}$ (dotted line)

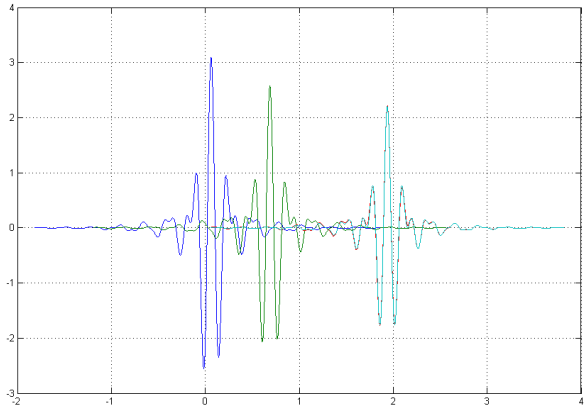

Figure 4: Functions $v_{3,0}$ (blue), $v_{3,5}$ (green), $v_{3,15}$ (cyan) and $2\pi h_2(x_{3,15}, 1.5\pi 8)\psi_{3,0}$ (dotted line)

Regarding the matrix M^j, we remark that we do not need to calculate v_{jk} since what we actually need are the values in (13). In Figure 5 we observe that the matrix are diagonal dominant, as expected.

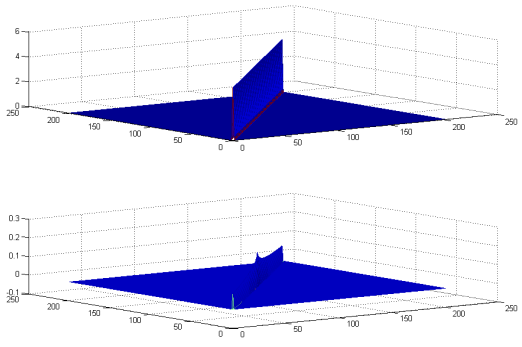

Figure 5: Matrix M^3 for h_1 (above) and h_2 (below)

4.2 Approximation scheme

The whole proposed approximation scheme is implemented in the following example. We construct a solution to IP associated to the operator with regular kernel

$$h_3(x,\omega) = \frac{1}{(1+3|x|^{0.5}+|\omega|)^{0.5}}, \quad |x| < 4.$$

We choose the function data g as the image through A of the sampled function

$$f(x) = e^{-x^2/2}(\sin(8\pi x) + \sin(4\pi x)).$$

Both plots of f and g are displayed in Figure 6.

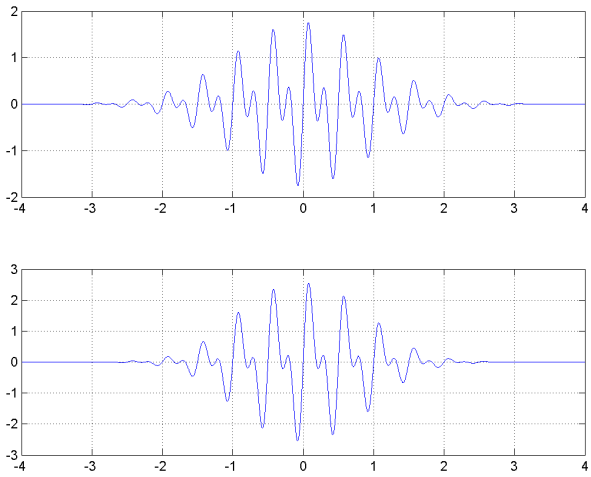

Figure 6: Functions f (above) and g (below)

Wavelet analysis indicates that the energy of the data g is concentrated in the subspaces W_1, W_2 and W_3, since levels $j = 1, 2, 3$ summarize the 10.84%, 55.96% and 33.20% of it, (see Table 1).

level$j$	energy	frequencies
5	0.0000	[100.5, 201.0]
4	0.0000	[50.2, 100.5]
3	0.3320	[25.1, 50.2]
2	0.5596	[12.5, 25.1]
1	0.1084	[6.28, 12.5]
0	0.0000	[3.14, 6.28]

Table 1: Energy distribution of g

Similarly for f, the energy is concentrated in the subspaces W_1, W_2 and W_3, (see Table 2). In this case, $A(\cup_{j=1}^{3} W_j) \subset \cup_{j=1}^{3} W_j$.

level j	energy	frequencies
5	0.0000	[100.5, 201.0]
4	0.0000	[50.2, 100.5]
3	0.4835	[25.1, 50.2]
2	0.4558	[12.5, 25.1]
1	0.0607	[6.28, 12.5]
0	0.0000	[3.14, 6.28]

Table 2: Energy distribution of f

In Figures 7, 8 and 9 we observe the diagonal dominant matrix M^j, $j = 1, 2, 3$ and their inverse.

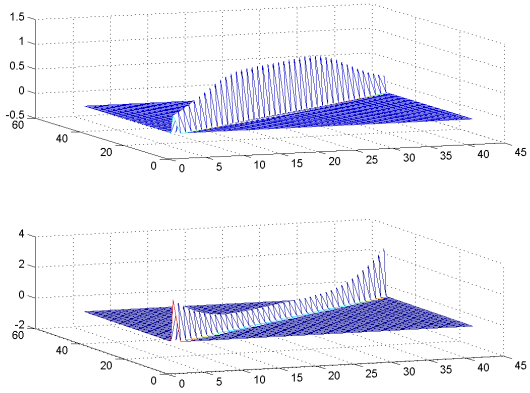

Figure 7: Matrix M^3 for h_3 (above) and its inverse (below)

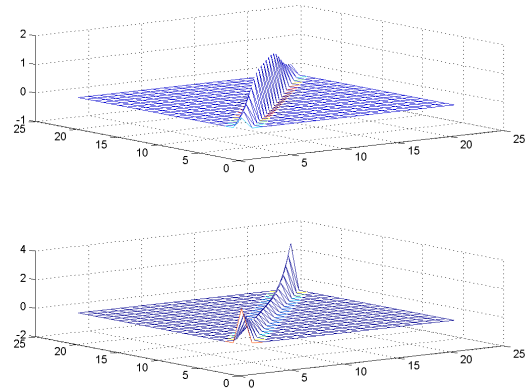

Figure 8: Matrix M^2 for h_3 (above) and its inverse (below)

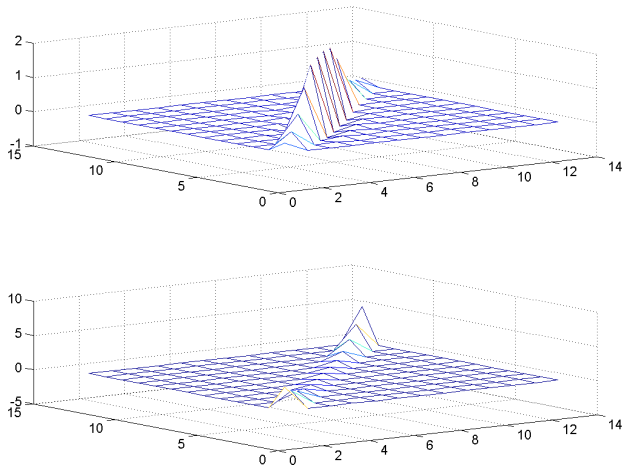

Figure 9: Matrix M^1 for h_3 (above) and its inverse (below)

In order to illustrate the procedure, we exhibit in Figure 10, the coefficients c_{jk} of g_j and b_{jk} of $\tilde{f}_j$, respectively.

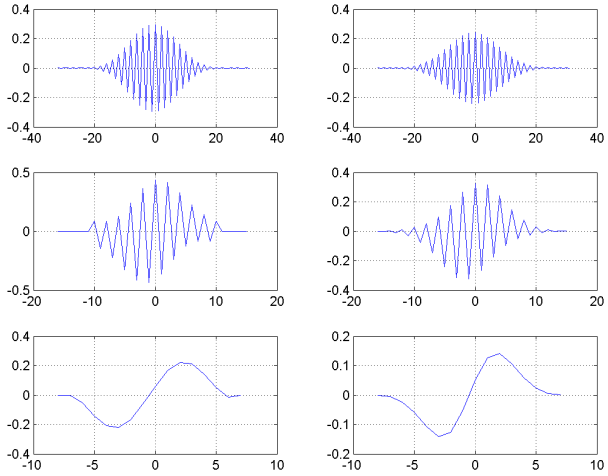

Figure 10: Coefficients of g_j (left) and $\tilde{f}_j$, $j = 1, 2, 3$ (right), (from below to above)

Finally, the sum of the reconstruction components $\sum_{j=1}^{3} \tilde{f}_j$, i.e., the approximate solution to the IP obtained with the proposed methodology is displayed in Figure 11, along with the projections of the real solution $\sum_{j=1}^{3} f_j$.

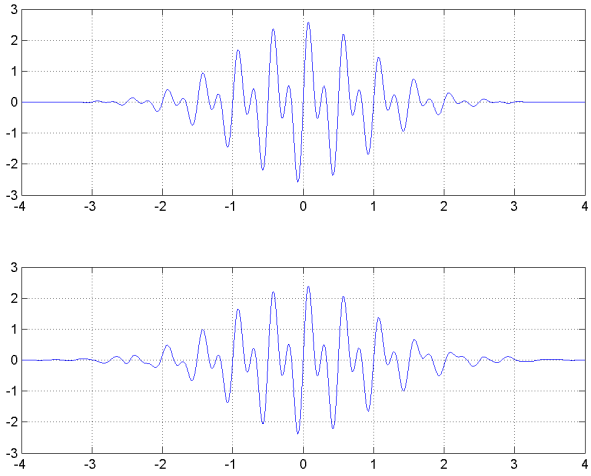

Figure 11: $\sum_{j=1}^{3} \tilde{f}_j$ (above) vs $\sum_{j=1}^{3} f_j$ (below)

5 CONCLUSIONS

In this work we have constructed approximate solutions to Inverse Problem $Af = g$ associated to integral operators A with regular kernel h. It consists in finding f for a given g.

For a fixed j, we first choose an appropriate wavelet basis $\{\psi_{jk},\ k \in \mathbb{Z}\}$, and project the data g into adequate wavelet subspaces, $\tilde{g}_j = \sum_{k\in\mathbb{K}_j} c_{jk}\psi_{jk}$. Afterwards we look for the images v_{jk} of the basis, $A\psi_{jk} = v_{jk}$. If $f = \sum_{j,k\in\mathbb{Z}} b_{jk}\psi_{jk}$, we calculate the vector coefficients $\mathbf{b}_k^j$ inverting a Grammian type matrix M^j. Finally, on each level $0 \leq j \leq J$, $\tilde{f}_j = \sum_{k\in\mathbb{K}_j} b_{jk}\psi_{jk}$ and $\tilde{f} = \sum_{0\leq j\leq J} \tilde{f}_j$ is the proposed approximate solution to the IP.

We observe that we only need to calculate the coefficients of the data and the elements of the matrix to obtain the vector $\mathbf{b}_\mathbf{k}^\mathbf{j}$ and build the solution component $\tilde{f}_j$.

Since we work with band limited wavelets, we regularized the problem when performing the projections to compact subsets in the frequency domain. Approximation errors are introduced when we truncate the projection of the data on each level j and in the calculation of the coefficients of f_j. Based on the properties of the operator and of the chosen wavelet basis, both errors can be handled and controlled.

The proposed approximation scheme is implemented on an example.

We remark that there is no general theory for integral equations of this type and only approximate solutions can be obtained. Ad-hoc approximation schemes must be developed taking into account particular properties of the kernel of the operator.

ACKNOWLEDGMENT

This work was partially supported by MINCyT- CONICET- CNRS (International Cooperation Programme, CONICET Resol. 147/15) and SOARD-AFOSR Grant FA9550-14-1-0276.

REFERENCES

A. Cohen M.H. and Reiβ M. Adaptive wavelet galerkin methods for inverse problems. *SIAM J. Numer. Anal.*, 42:1479–1501, 2004.

Dicken V. and Maaβ P. Wavelet-galerkin methods for ill-posed problems. *J. Inv Ill-Posed Problems*, 4:203–222, 2006.

Donoho D. Nonlinear solution of linear inverse problems by wavelet-vaguelet decomposition. *Applied and Computational Harmonic Analysis*, 49, 1995.

Kress R. *Linear Integral Equations. Applied Mathematical Sciences*. Springer, 2014.

Mallat S. *A Wavelet Tour of Signal Processing*. S. Mallat, 2009.

Meyer Y. Ondelettes et operateurs 2. operatteurs de calderon zygmund. *Hermann et Cie*, 1990.

Serrano E., Troparevsky M., and Fabio M. Wavelet-vaguelet decomposition methods to solve pseudodifferential inverse problems. *Proceedings SIMMAC*, 2012.

Serrano E., Troparevsky M., and Fabio M. Solving deconvolution type problems by wavelet decomposition methods. *Journal of Contemporary Mathematical Analysis*, 49, 2014a.

Serrano E., Troparevsky M., and Fabio M. Wavelet projection methods for solving pseudodifferential inverse problems. *Internaional Journal of Waveletes Multiresolution and Information Processing*, 12:14500251–17, 2014b.

Walnut D.F. *An Introduction to Wavelet Analysis. Applied and Numerical Harmonic Analysis*. Birkhauser, 2002.